Cellular Senescence Is Associated With Human Retinal Microaneurysm Formation During Aging

Mariana López-Luppo,[1,2] Joana Catita,[1,2] David Ramos,[1,3] Marc Navarro,[1,2] Ana Carretero,[1,2] Luísa Mendes-Jorge,[1,3,4] Pura Muñoz-Cánoves,[5] Alfonso Rodriguez-Baeza,[6] Victor Nacher,[1,2] and Jesus Ruberte[1–3]

[1]Center of Animal Biotechnology and Gene Therapy, Universitat Autònoma de Barcelona, Bellaterra, Spain
[2]Department of Animal Health and Anatomy, School of Veterinary Medicine, Universitat Autònoma de Barcelona, Bellaterra, Spain
[3]Interdisciplinary Centre of Research in Animal Health, Faculty of Veterinary Medicine, Universidade de Lisboa, Lisbon, Portugal
[4]Department of Morphology and Function, Faculty of Veterinary Medicine, Universidade de Lisboa, Lisbon, Portugal
[5]Cell Biology Group, Department of Experimental and Health Sciences, Pompeu Fabra University. Institució Catalana de Recerca i Estudis Avançats (ICREA), Barcelona, Spain
[6]Department of Morphological Sciences, School of Medicine, Universitat Autònoma de Barcelona, Bellaterra, Spain

Correspondence: Jesús Ruberte, Center of Animal Biotechnology and Gene Therapy, Edifici H, Universitat Autònoma de Barcelona, Bellaterra 08193, Spain; jesus.ruberte@uab.es.

ML-L and JC contributed equally to the work presented here and should therefore be regarded as equivalent authors.

Submitted: July 12, 2016
Accepted: April 17, 2017

Citation: López-Luppo M, Catita J, Ramos D, et al. Cellular senescence is associated with human retinal microaneurysm formation during aging. *Invest Ophthalmol Vis Sci*. 2017;58:2832–2842. DOI:10.1167/iovs.16-20312

Purpose. Microaneurysms are present in healthy old-age human retinas. However, to date, no age-related pathogenic mechanism has been implicated in their formation. Here, cellular senescence, a hallmark of aging and several age-related diseases, has been analyzed in the old-age human retina and in the retina of a progeric mouse.

Methods. Retinas were obtained from 17 nondiabetic donors and from mice deficient in Bmi1. Cellular senescence was analyzed by immunohistochemistry, senescent-associated β-galactosidase activity assay, Sudan black B staining, conventional transmission electron microscopy, and immunoelectronmicroscopy.

Results. Neurons, but not neuroglia, and blood vessels undergo cellular senescence in the old-age human retina. The canonical senescence markers p16, p53, and p21 were up-regulated and coexisted with apoptosis in old-age human microaneurysms. Senescent endothelial cells were discontinuously covered by fibronectin, and p16 colocalized with the β_1 subunit of fibronectin receptor $\alpha_5\beta_1$ integrin under the endothelial cellular membrane, suggesting anoikis as a mechanism involved in endothelial cell apoptosis. In a progeric mouse model deficient in Bmi1, where p21 was overexpressed, the retinal blood vessels displayed an aging phenotype characterized by enlarged caveolae and lipofuscin accumulation. Although mouse retina is not prone to develop microaneurysms, Bmi1-deficient mice presented abundant retinal microaneurysms.

Conclusions. Together, these results uncover cellular senescence as a player during the formation of microaneurysms in old-age human retinas.

Keywords: retina, microaneurysms, cellular senescence, p16, p53, p21

Microaneurysms are focal dilations of capillaries most frequently seen in the retina, although they can also be found in other organs, such as kidney and heart.[1,2] Capillary microaneurysms are a clinicopathologic hallmark of human diabetic retinopathy,[3–7] but they are also present in healthy old-age human retinas.[8,9] Several mechanisms have been implicated in retinal microaneurysm formation during diabetes, including cell death, impaired angiogenesis, changes in intraluminal rheology, and basement membrane alterations.[10–14] However, to date, little is known about the mechanisms involved in the formation of age-related retinal microaneurysms and whether these mechanisms are different from those occurring during diabetes.

Cellular senescence is one of the hallmarks of aging and can be defined as a stable arrest of the cell cycle.[15–17] Recently, it has been proposed that the central purpose of cellular senescence is to initiate a sequence of processes that eliminate damaged cells and culminate in tissue regeneration.[18] This beneficial process can be corrupted, particularly in aged tissues, leading to an accumulation of senescent cells that may aggravate tissue dysfunction through a senescence-associated phenotype, which is particularly enriched in proinflamatory cytokines and matrix metalloproteinases.[17,19] Several vascular pathologies have been associated with cellular senescence, including brain and coronary aneurysms among others.[20,21] However, the overall effect of senescence during the aneurysm formation is not well understood.

The main objectives of this study were (1) to analyze cellular senescence in the old-age human retina and (2) to explore whether senescence is implicated in the formation of retinal microaneurysms during aging. Here we confirm that cellular senescence occurred in old-age human retinas. Retinal neurons but not neuroglia cells underwent cellular senescence during aging. In addition, blood vessels displayed a senescent

phenotype characterized by p16, p53, p21, and p62 overexpression, senescent-associated β-galactosidase (SA-β-gal) activity, and accumulation of lipofuscin. In comparison with senescent capillaries, p16, p53, and p21 were up-regulated in microaneurysms. Apoptosis and cellular senescence co-occurred in retinal microaneurysms of old-age human retinas. Senescent endothelial cells expressed p16 in the inner part of their cellular membrane, where p16 colocalized with the β_1 integrin subunit. In addition, fibronectin of the basement membrane coated discontinuously the abluminal surface of senescent endothelial cells. All together, these data could suggest that p16 induces anoikis by direct interaction with the fibronectin receptor $\alpha_5\beta_1$ integrin. To get further insight into the age-mediated mechanisms implicated in microaneurysm formation, retinas from a progeric mouse model deficient in Bmi1 that overexpress p21 were analyzed. Retinal blood vessels in *Bmi1*$^{-/-}$ mice displayed an aging phenotype characterized by enlarged caveolae and accumulation of lipofuscin granules. Although retinal microaneurysms do not generally develop in mouse models, *Bmi1*$^{-/-}$ mice showed abundant microaneurysms in their retinal superficial vascular plexus. The presence of retinal microaneurysms in *Bmi1*$^{-/-}$ mice reinforces the hypothesis that cellular senescence is associated with the pathogenesis of retinal microaneurysms in elderly people.

Materials and Methods

Human Retinas

Human eye samples were obtained from voluntary body donations to the Faculty of Medicine at Universitat Autònoma de Barcelona (UAB). The procedure of body donation was in accordance with the Catalonian law (DECRET 297/1997, de 25 de Novembre) and was approved on March 27, 2015 by the ethics committee Comisió d'Ètica en l'Experimentació Animal i Humana (CEEAH/UAB). All participants in the study gave, during their lifetime, written consent for donation of their bodies after death for teaching and research purposes. Our laboratory received human eye samples without knowledge of the donor's identity. Only biological data, such as sex, age, clinical history, and cause of death, were available (Table). Eyes were obtained from 17 donors: 14 old-age donors ($\bar{X} = 85.28$ years old) and 3 middle-age donors ($\bar{X} = 40$ years old). Corneas were removed, and retinas were examined using a dissecting microscope for pathologic evidence of neovascularization. None of the donors had history of diabetic disease (Table), nor did they present characteristic lesions of diabetic proliferative retinopathy. However, the possibility of undiagnosed asymptomatic nonproliferative diabetic retinopathy cannot be ruled out in this pool of old-age donors. Eyes were fixed in a solution of paraformaldehyde 4% with picric acid in 0.01 M PBS for 24 hours. Time between death and fixation was critical to obtain adequate samples for immunohistochemistry and electron microscopy. The average time for fixation in our study was 7 hours (Table). Next, eyes were washed in PBS, partially dehydrated, and maintained in a 70% alcohol solution at 4°C. The storage of prefixed eyes in this cold alcoholic solution allowed to perform immunohistochemistry and electron microscopy during a long period of time. For their immunohistochemical analysis, retinal fragments of about 3 mm^2 were dissected out from the prefixed eyes and processed adequately for each experiment.

Animals

Two-month-old *Bmi1*$^{-/-}$ *Rd1* mice, yielded from P. Muñoz-Cànoves (Cell Biology Group, Department of Experimental and Health Sciences, Pompeu Fabra University), were generated by intercrossing heterozygotes (*Bmi1*$^{+/-}$) in a FVB/NJ background. *Bmi1*$^{+/+}$ *Rd1* littermates were used as controls. Animal care and experimental procedures were performed according to the ARVO Statement for the Use of Animals in Ophthalmic and Vision Research and were approved by CEEAH/UAB (Permit 1666).

Table. Sex, Age, Cause of Death, and Time Between Death and Eye Fixation

No.	Sex	Age, y	Cause of Death	Time Between Death and Fixation, h
1	Female	89	Cardiopulmonary arrest	5.5
2	Male	83	Cardiopulmonary arrest	8
3	Female	86	Cardiopulmonary arrest, aspiration pneumonia	3
4	Male	99	Cardiopulmonary arrest	9.5
5	Male	85	Cardiopulmonary arrest, dilated cardiomyopathy	4.5
6	Male	88	Cardiopulmonary arrest, pneumonia	7
7	Male	86	Cardiopulmonary arrest	6.5
8	Female	80	Cardiopulmonary arrest, hepatic neoplasia	NA
9	Male	91	Cardiopulmonary arrest, gastric neoplasia	12
10	Female	34	Cardiopulmonary arrest, brain tumor	7
11	Female	88	Peritoneal neoplasia, multiple organ failure	8
12	Male	88	Cardiopulmonary arrest, stroke	8
13	Male	72	Liver failure, hepatic cirrhosis	7.5
14	Female	42	Cardiopulmonary arrest	NA
15	Female	83	Cardiopulmonary arrest	8.5
16	Female	76	Cardiopulmonary arrest, hypertension	3.5
17	Female	44	Cardiopulmonary arrest, postanoxic encephalopathy	9

NA, not available.

Immunohistochemistry

Retinal fragments from all donors were used for immunohistochemistry (Table). Paraffin-sections and whole mount retinas were incubated overnight at 4°C with the following antibodies: mouse anti-p16 (Santa Cruz Biotechnology, Santa Cruz, CA, USA) at 1:50 dilution; mouse anti-p53 (Abcam, Cambridge, UK) at 1:100 dilution; rabbit anti-p21 (Abcam) at 1:100 dilution; rabbit anti-protein gene product 9.5 (PGP) (DakoCytomation, Glostrup, Denmark) at 1:350 dilution; rabbit anti-parvalbumin at 1:100 dilution; rabbit anti-glutamine synthetase (GS) (Sigma-Aldrich Corp., St. Louis, MO, USA) at 1:500 dilution; rabbit anti–glial fibrillary acidic protein (GFAP) (DakoCytomation) at 1:1000 dilution; goat anti-collagen IV (Millipore, Temecula, CA, USA) at 1:20 dilution; rabbit anti-activated caspase3 (Cell Signaling Technology, Inc., Danvers, MA, USA) at 1:250 dilution; rabbit anti-integrin β1 subunit (Abcam) at 1:100 dilution; rabbit anti-fibronectin (BD Pharmigen, San José, CA, USA) at 1:100 dilution, and rabbit anti-p62 (Abcam) at 1:100 dilution. After they were washed in PBS, retinas were incubated at 4°C overnight with specific secondary antibodies: biotinylated anti-mouse IgG (Vector Laboratories, Burlingame, CA, USA) at 1:100 dilution; anti-goat IgG Alexa 568 (Invitrogen, Carlsbad, CA, USA) at 1:250 dilution, and anti-rabbit IgG Alexa

568 (Invitrogen) at 1:250 dilution. For fluorescence visualization, streptavidin Alexa Fluor 488 (Invitrogen) at 1:100 dilution was used. Nuclear counterstaining was performed with To-Pro-3 iodide (Invitrogen) at 1:100. Lipofuscin autofluorescence was analyzed using an excitation laser of 488 nm. The activated caspase 3 signal associated with the lipofuscin autofluorescence was visualized with streptavidin Cy5.5 (Invitrogen) at 1:500 dilution. Nuclei in this experiment were counterstained with Hoechst stain (Sigma-Aldrich Corp.) at 1:100 dilution. Slides were mounted into Fluoromount mounting medium (Sigma-Aldrich Corp.) for microscopic analysis using a laser scanning confocal microscope (TCS SP2, Leica Microsystems GmbH, Heidelberg, Germany).

SA-β-gal Assay

SA-β-gal activity was checked as previously described.[22] Briefly, whole mount retinas were fixed at room temperature for 15 minutes in 0.5% glutaraldehyde/PBS (pH 6.0). After fixation, retinas were washed twice in PBS (pH 6.0) and incubated in the X-gal solution at pH 6.0 (5 mM potassium ferrocyanide, 5 mM potassium ferricyanide, 1 mM $MgCl_2$ in PBS solution, pH 7.5) containing 1 mg/ml X-gal (5-bromo-4-chloro-3-indolyl β-D-galactopyranoside) (Sigma-Aldrich Corp.) at 37°C overnight. In parallel, as a control of the technique, β-gal activities were assayed in X-gal solution at pH 4.0 and 7.5. Samples were checked during incubation and the reaction was stopped approximately after 3 hours, when SA-β-gal activity was evident in samples at pH 6 with no change in β-gal activity at pH 7.5. Samples were washed several times in PBS to eliminate the X-gal solution and immediately photographed using a stereo microscope (SMZ 1000; Nikon, Tokyo, Japan) fitted with a high-resolution camera (DXM 1200F; Nikon).

Sudan Black B Staining

Paraffin-embedded retinal sections were dewaxed with xylene, rehydrated until 70% ethanol, and stained with Sudan black B (SBB) solution containing 0.7 g SBB (Sigma-Aldrich Corp.) dissolved in 70% ethanol, for 2 to 8 minutes at room temperature. Slides were then immersed into 50% ethanol, washed in distilled water, counterstained with 0.1% Nuclear Fast Red (Aldrich Chem. Co., Milwaukee, WI, USA), and mounted into 40% glycerol/Tris-buffered saline medium for microscopic analysis using an optical microscope (Eclipse E-800; Nikon) and a Nikon digital camera (DXM 1200F; Nikon).

Transmission Electron Microscopic Analysis

Retinal fragments of 1 mm^2 were fixed in 2.5% glutaraldehyde and 2% paraformaldehyde for 2 hours at 4°C. After washing in cold phosphate buffer, samples were postfixed in 1% osmium tetroxide, dehydrated through a graded acetone series, and embedded in epoxy resin. Ultrathin sections (70 nm) from resin blocks were stained using lead citrate and 2% uranyl acetate followed by examination in a transmission electron microscope (H-7000; Hitachi Ltd., Tokyo, Japan).

For immunoelectronmicroscopy, after fixation (0.1% glutaraldehyde and 4% paraformaldehyde) and rinsing in 150 mM ammonium chloride, retinal fragments were cryoprotected in increasing concentrations of sucrose (0.5 to 2.3 M) for 3 days. Samples were maintained in liquid nitrogen until cryosubstitution in pure methanol at gradually increasing temperatures from −120°C to −30°C for 4 days with Leica EM AFS2 (Leica, Vienna, Austria). Infiltration was achieved by embedding the retinal fragments in resin Lowicryl K4M (EMS, Hatfield, PA, USA) gradually diluted in methanol at −30°C overnight, following UV polymerization for 48 hours at −30°C. Ultrathin retinal sections (70 nm) from resin blocks were first blocked in PBS containing 20 mM glycine and 1% bovine serum albumin (BSA), followed by incubation with primary mouse antibody against $p16^{INK4a}$ (Santa Cruz Biotechnology) diluted at 1:10 in the same blocking solution at 4°C overnight. After washing in PBS containing 20 mM glycine, sections were incubated with an anti-mouse IgG 15-nm gold (BBI Solutions, Cardiff, UK) diluted 1:25 for 1 hour at room temperature and were washed in PBS and Milli-Q water. Grids were contrasted and examined in the same manner as sections for conventional transmission electron microscopy. To determine whether the gold complex is contributing to the labeling through unspecific bindings to the tissue, the primary antibody was omitted in the protocol.

In Situ Protein Quantification

To analyze p16 expression in the retina, mean fluorescence intensity (MFI) was measured in immunohistochemically labeled retinal paraffin sections of a middle- and an old-aged donor. To measure the expression of activated caspase 3 and the senescence markers p16, p53, and p21 in the microaneurysms, two-dimensional projections of stacks of confocal images were obtained from old-age whole mount retinas by optical sectioning at successive x-y focal planes with a 1 μm vertical step through the entire vessel depth. MFI was measured in 5 to 10 randomly selected microaneurysms and in adjacent areas of nonaffected capillaries from two different aged donors.

Values of MFI were obtained with the Leica LAS AF Lite imaging software according to the equation: $\mathrm{MFI} = \frac{\sum^{i}(p)}{np}$, where $i(p)$ is the intensity of a pixel within the confocal plane, and $n(p)$ is the total number of pixels of the plane. Results are reported in gray values, fluorescent intensity arbitrary units.

Identical image acquisition parameters were applied to all the experiments, which provided comparable images across the different experiments.

Statistical Analysis

Results were expressed as mean ± SD. Differences between groups were evaluated by paired or unpaired Student's *t*-test, as appropriate. $P < 0.05$ was considered significant.

Results

Cellular Senescence in Old-Age Human Retinas

To determine the cellular type and topography of senescent cells in human retinas, the expression of p16, a well-established cellular senescence biomarker,[23] was analyzed in immunolabeled paraffin-embedded retinal sections from middle-age and old-age donors. Our results revealed increased p16 expression throughout all retinal layers in old-age donors (Fig. 1). As an example, quantification of protein fluorescence intensity in a retina from an 85-year-old donor showed that p16 expression was nearly 12 times higher in comparison with a retina from a 42-year-old donor (8.63 fluorescence intensity arbitrary units versus 0.72 fluorescence intensity arbitrary units, respectively). This difference in p16 expression between middle- and old-age human retinas correlates with the variations of p16 expression observed by other authors when comparing young and old tissues.[24]

In addition, subcellular localization of p16 changed during aging. Middle-age retinas showed exclusively nuclear p16 expression (Fig. 1A), whereas in old-age retinas, p16 localization was both nuclear and cytoplasmic (Figs. 1B, 2). Positive

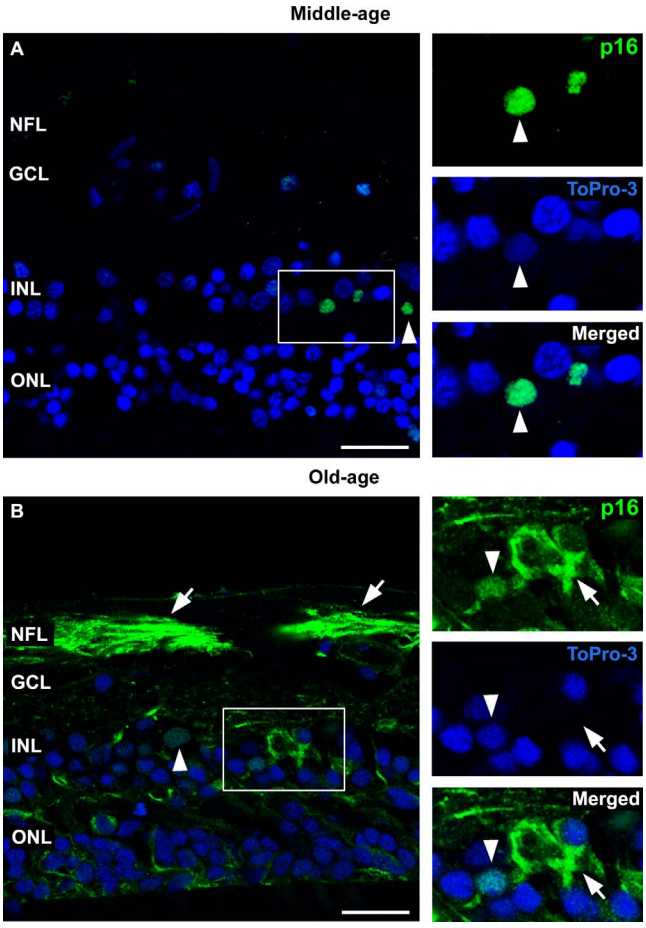

Figure 1. Old-age human retinas overexpressed p16. (**A**) Immunohistochemical detection of p16 in paraffin sections from middle-age retinas showed that this protein was only present in few nuclei (*arrowheads*) in the inner nuclear layer. (**B**) In contrast, in old-age retinas, p16 was several times overexpressed in both the nuclei (*arrowheads*) and cytoplasm (*arrows*) of cells located in all retinal layers, especially in the nerve fiber layer. Nuclei were counterstained with ToPro-3 (*blue*). NFL, nerve fiber layer; GCL, ganglion cell layer; INL, inner nuclear layer; ONL, outer nuclear layer. *Scale bars* denote **A** = 23.2 μm and **B** = 17.02 μm.

p16 immunoreaction has been described in the nucleus or both in the nucleus and the cytoplasm.[25] However, according to most investigators, p16 staining exclusively seen at cytoplasmic level should be interpreted as false-positive signal.[25]

To further investigate which type of retinal cells expressed p16 in old-age retinas, double immunohistochemistry in paraffin-embedded retinal sections was done. Immunolabeling with anti-protein gene product (PGP) 9.5 antibody, a useful marker for human ganglion cells and cones,[26] confirmed the expression of p16 in ganglion cells and rods (Fig. 2A). Ganglion cells expressed p16 in their nuclei and cytoplasm, especially at the level of their axons, which form the retinal nerve fiber layer (Figs. 2A, 3B). Rods only expressed p16 in their nuclei (Fig. 2A). Furthermore, as evidenced by immunolabeling against parvalbumin, horizontal cells expressed p16, both in their nuclei and cytoplasm, and amacrine cells expressed p16 only in their nuclei (Fig. 2B). In contrast with retinal neurons, neuroglial retinal cells did not express p16 in old-age retinas (Figs. 2C, 2D). Neither astrocytes marked with GFAP[27] nor Müller cells marked with GS,[28] which only expressed p16 in their cytoplasm, showed specific immunostaining for p16.

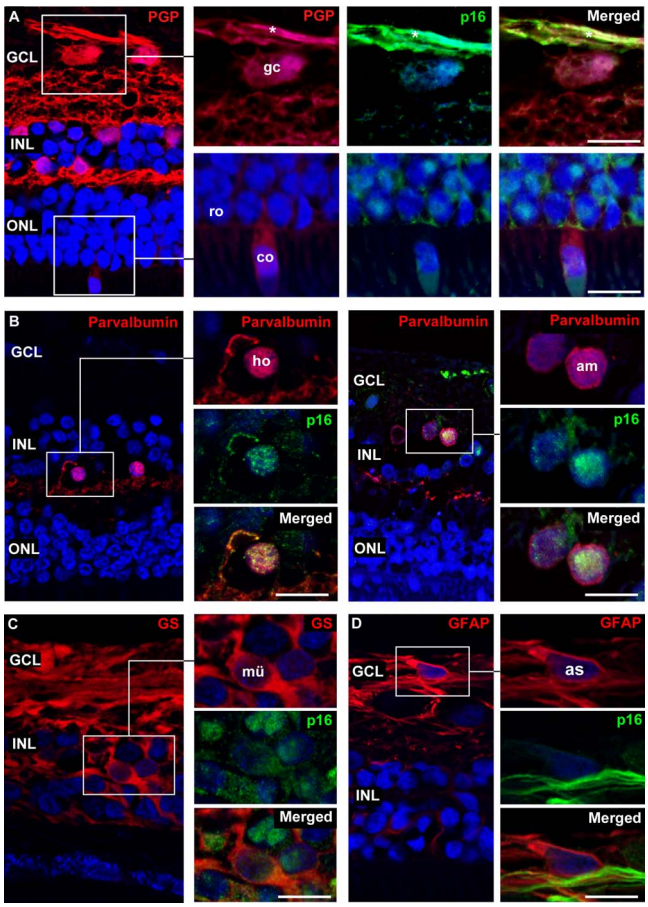

Figure 2. Characterization of retinal cells overexpressing p16 in old-age human retinas. (**A**) Retinal sections immunostained with PGP, showed $p16^{INK4a}$ in the nuclei, cytoplasm, and especially in the axons (*asterisk*) of ganglion cells (gc). Rod (ro) nuclei, but not cone (co) nuclei expressed $p16^{INK4a}$. (**B**) Retinal sections immunostained with parvalbumin, showed $p16^{INK4a}$ in the nuclei and cytoplasm of horizontal cells (ho) and only in the nuclei of amacrine cells (am). Retinal sections immunostained with GS (**C**) and GFAP (**D**) did not show a specific expression of $p16^{INK4a}$ in Müller cells (mü) and astrocytes (as). Nuclei were counterstained with ToPro-3 (*blue*). GCL, ganglion cell layer; INL, inner nuclear layer; ONL, outer nuclear layer. *Scale bars* denote **A** (*upper inset*) = 11.66 μm; **A** (*bottom inset*) = 10.91 μm; **B** (*left inset*) = 9.69 μm; **B** (*right inset*) = 9.20 μm; **C** = 13.58 μm; and **D** = 8.44 μm.

Cellular Senescence in Old-Age Human Retinal Blood Vessels

To analyze cellular senescence in retinal blood vessels, we performed double immunostaining of whole mount retinas with anti-p16, anti-p53, and anti-p21 antibodies, together with an antibody against collagen IV to evidence blood vessel basement membrane.[29] In comparison with middle-age retinal blood vessels, which did not express senescence biomarkers, old-age retinal blood vessels intensely expressed p16, p53, and p21 (Figs. 3–5). As previously discussed, subcellular localization of p16 changed from nuclear to both nuclear and cytoplasmic during aging. As expected, a more detailed analysis revealed that p16 was found in the nuclei and cytoplasm of cells of the vascular wall (Fig. 3C). This was consistent with studies performed in other tissues besides the retina that showed an age-dependent increase of p16 expression in endothelial cells[30] and vascular smooth muscle cells[31] during aging.

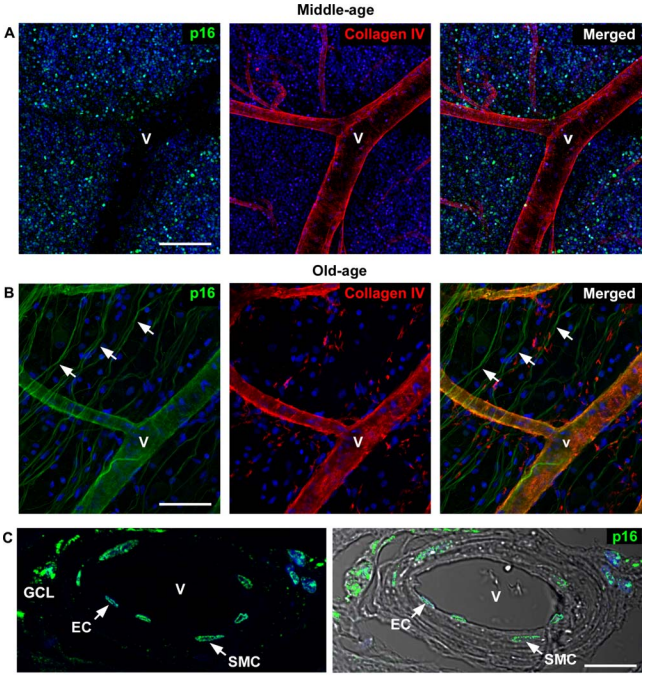

FIGURE 3. Old-age human retinal blood vessels overexpress p16. (**A**) Blood vessels did not express $p16^{INK4a}$ in middle-age retinas. (**B**) In contrast, blood vessels overexpressed $p16^{INK4}$ in old-age retinas. (**C**) Both, nuclei and cytoplasm of endothelial and smooth muscle cells overexpressed $p16^{INK4}$ in old-age retinal blood vessels. **A** and **B** are whole mount retinal preparations, where blood vessels were marked with anti–collagen IV antibody. **C** is a retinal section where the vessel morphology is recognizable by the transmission light mode. Nuclei were counterstained with ToPro-3 (*blue*). V, blood vessel (arteriole); GCL, ganglion cell layer; EC, endothelial cell; SMC, smooth muscle cell; *arrows,* axons of ganglion cells. *Scale bars* denote **A** = 114.87 μm; **B** = 67.95 μm; and **C** = 39.82 μm.

Although p16, p53, and p21 are considered canonical biomarkers for cellular senescence,[18] SA-β-gal histochemistry, the most widely used assay for senescence,[32] was also performed in old-age retinas. Specific SA-β-gal activity, β-gal

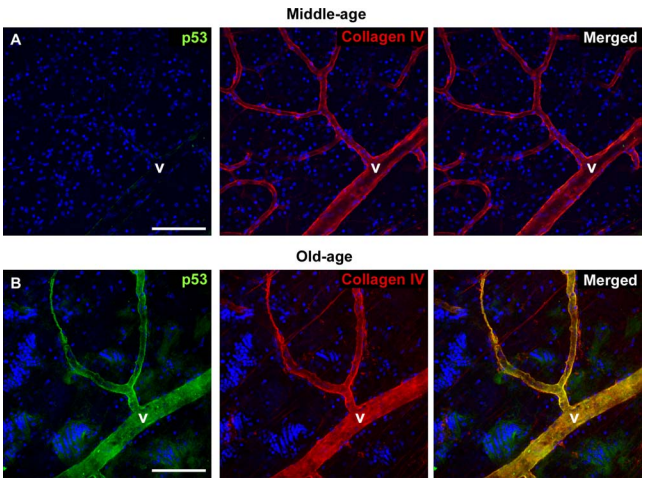

FIGURE 4. Old-age human retinal blood vessels overexpress p53. (**A**) Immunohistochemistry in whole mount retinas demonstrated that p53 is not expressed in middle-age retinal blood vessels. (**B**) In contrast, p53 was consistently expressed in old-age retinal blood vessels. Nuclei were counterstained with Hoechst stain. V, blood vessel (arteriole). *Scale bars* denote 241.68 μm.

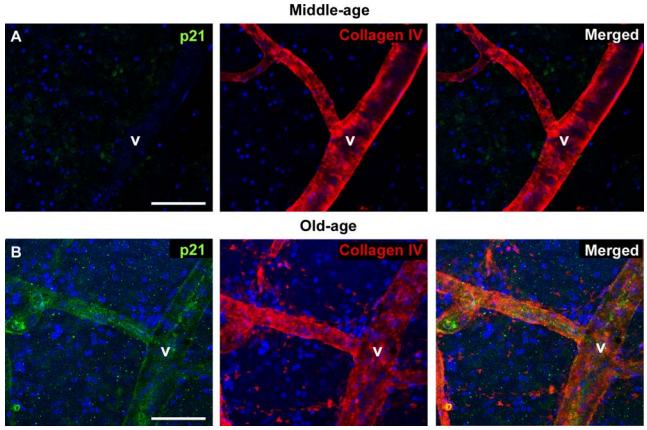

FIGURE 5. Old-age human retinal blood vessels overexpress p21. (**A**) Immunolabeling of p21 in whole mount retinas demonstrated that middle-age retinal blood vessels do not express this protein. (**B**) In contrast, p21 expression was detected in old-age retinal blood vessels. Nuclei were counterstained with Hoechst stain (*blue*). V, blood vessel (arteriole). *Scale bars* denote 67.9 μm.

enzymatic activity at suboptimal pH (pH 6.0), was observed in endothelial and smooth muscle cells of aged retinal blood vessels (Fig. 6A). As expected, no staining of β-gal at pH 7.5 and intense staining of β-gal at pH 4.0 were observed in old-age retinas (Fig. 6B).

Recently, SBB staining for lipofuscin has been recognized as a new method to detect cellular senescence.[33] Similarly to SA-β-gal activity, which is based on the increased lysosomal content of senescent cells,[34] lipofuscin is a pigment that aggregates with age in cellular lysosomes.[35–37] To corroborate cellular senescence, we used this new method and, as expected, old-age retinal blood vessels were positively stained by SBB (Fig. 7). This confirmed previous results of our group that showed lipofuscin granules in aged human retinal blood vessels using transmission electron microscopy.[9]

It has been suggested that autophagy mediates the acquisition of the senescence phenotype.[38] Sequestosome-1, p62, an adaptor protein involved in the delivery of ubiquitin-bound cargo to the autophagosome,[39] is up-regulated during senescence,[38] and it has been seen coexpressed with p16 in

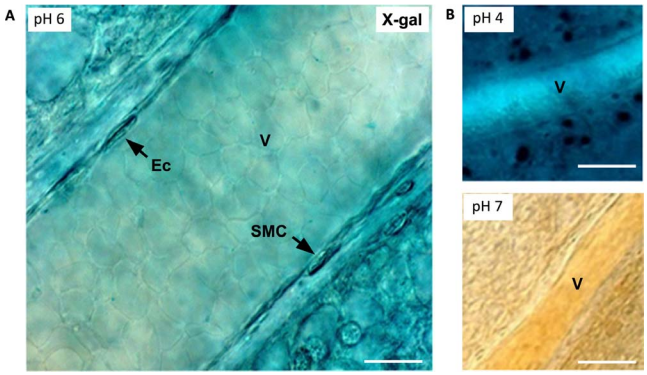

FIGURE 6. Specific SA-β-gal activity was observed in old-age human retinal blood vessels. (**A**) Endothelial and smooth muscle vascular cells exhibited β-galactosidase enzymatic activity at suboptimal pH 6.0, indicating that old-age retinal blood vessels undergo cellular senescence. (**B**) β-Galactosidase activity was also evaluated at pH 4.0 and 7.5. As expected, no activity was observed at pH 7.5 and intense activity was observed at pH 4.0. V, blood vessel (venule); EC, endothelial cell; SMC, smooth muscle cell. *Scale bars* denote **A** = 73.13 μm and **B** = 410.5 μm.

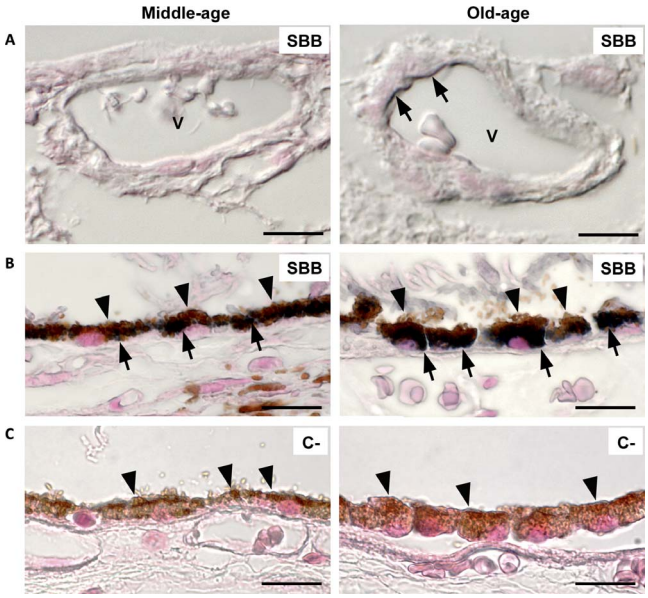

FIGURE 7. Lipofuscin was accumulated in old-age human retinal blood vessels. (**A**) SBB (*arrows*) was observed in endothelial retinal cells from old-age donors but not in middle-age retinal blood vessels. (**B**) The staining specificity for lipofuscin was controlled at the retinal pigment epithelium, which content lipofuscin in healthy conditions in both middle- and old-age retinas. Lipofuscin black granules (*arrows*) stained by SBB are clearly differentiable from melanin brown granules (*arrowheads*) in retinal pigment epithelial cells. (**C**) Omission of SBB staining allowed to further distinguishing lipofuscin from melanin granules. Samples were counterstained with Nuclear Fast Red. V, blood vessel (arteriole); GCL, ganglion cell layer; Cho, choroid. *Scale bars* denote **A** (*left*) = 8.78 μm; **A** (*right*) = 6.80 μm; **B** (*left*) = 12.21 μm; **B** (*right*) = 14.25 μm; **C** (*left*) = 15.18 μm; and **C** (*right*) = 15.14 μm.

several pathologies.[40] Our results showed that, in comparison with middle-age retinas, p62 was overexpressed in the blood vessels of old-age retinas (Fig. 8), confirming the association between cellular senescence and altered autophagy in human retinal blood vessels during aging.

Taken together, the expression of p16, p53, and p21, SA-β-gal activity, and SBB staining, as well as overexpression of p62 found in old-age human retinal blood vessels, strongly suggested that they undergo cellular senescence during aging.

Cellular Senescence Was Up-Regulated in Old-Age Human Retinal Microaneurysms

We next assessed the expression pattern of p16, p53, and p21 in retinal microaneurysms. Double immunohistochemistries with anti-p16, anti-p53, and anti-p21antibodies, together with anti-collagen IV antibody, performed in whole mount retinas from old-age humans revealed an increased expression of p16, p53, and p21 in retinal microaneurysms compared with nonaffected adjacent capillary regions (Figs. 9–11). Moreover, an accurate quantification of mean fluorescence intensity in microaneurysms and their adjacent nonaffected capillary regions demonstrated that differences in the expression of p16 (74.7 ± 21.5 Gy in the microaneurysm versus 16.7 ± 5.4 Gy in the capillary wall), p53 (64.89 ± 21.06 Gy in the microaneurysm versus 35.41 ± 19.85 Gy in the capillary wall), and p21 (35.37 ± 17.38 Gy in the microaneurysm versus 23.11 ± 9.061 Gy in the capillary wall) were statistically significant ($P < 0.05$).

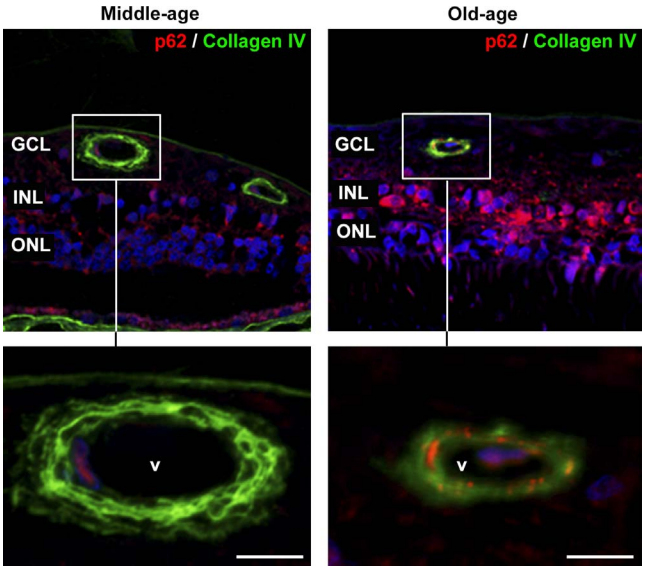

FIGURE 8. Sequestosome-1 (p62) was accumulated in old-age human retinal blood vessels. Immunohistochemical detection of p62 in retinal paraffin sections demonstrated that this protein was overexpressed in all layers and blood vessels of retinas from old-age donors in comparison to middle-age donors. Nuclei were counterstained with ToPro-3 (*blue*). V, blood vessel (arteriole); GCL, ganglion cell layer; INL, inner nuclear layer; ONL, outer nuclear layer. *Scale bars* denote *right* = 10.16 and *left* = 7.25 μm.

Cellular Senescence and Apoptosis Co-Occurred in Old-Age Retinal Microaneurysms

We previously reported that activated caspase 3, a well-recognized biomarker for apoptosis,[41] is present in retinal capillaries during aging.[9] Here we show that activated caspase 3 was increased in retinal microaneurysms compared with adjacent nonaffected capillary regions (Fig. 12A), suggesting that apoptosis of endothelial cells and pericytes is involved in microaneurysm formation during aging.

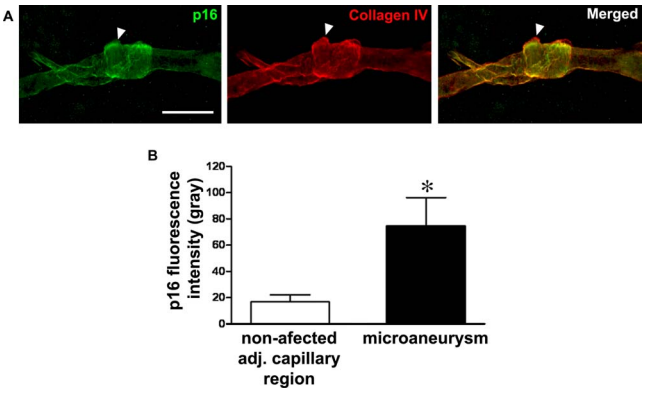

FIGURE 9. p16 was up-regulated in old-age human retinal microaneurysms. Microaneurysms, identified as localized dilations of retinal capillaries in collagen IV immunostained whole mount retinas, overexpressed $p16^{INK4a}$ in comparison with nonaffected adjacent capillary regions (**A**). Interestingly, the higher expression of $p16^{INK4a}$ coincided with areas of basement membrane thickening and alteration (*arrowhead*). (**B**) Quantification of fluorescence intensity in five different microaneurysms and their adjacent nonaffected capillaries demonstrated that differences in p16 expression were statistically significant. *$P < 0.05$. *Scale bars* denote **A** = 19.11 μm; **B** = 27.2 μm; **C** = 24.33 μm; **D** = 21.71; and **E** = 18.33 μm.

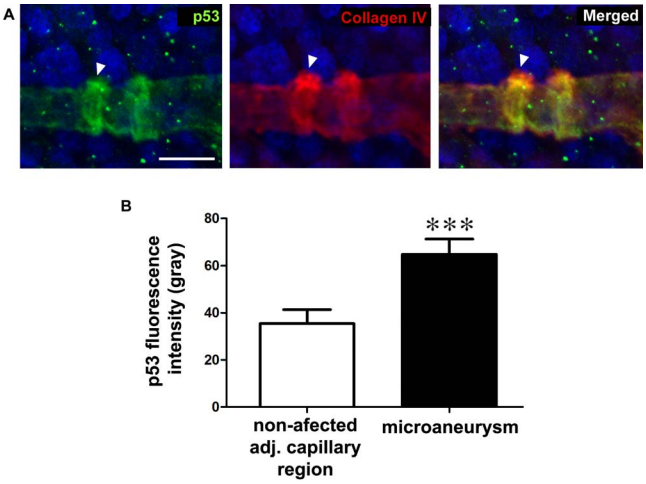

Figure 10. p53 was up-regulated in old-age human retinal microaneurysms. Double immunohistochemical detection of p53 (*green*) and collagen IV (*red*) in whole mount old-age retinas demonstrated an increase of p53 expression in microaneurysms compared with a nonaffected capillary region (**A**). Interestingly, the higher expression of p53 coincided with areas of basement membrane thickening and alteration (*arrowhead*). (**B**) Quantification of fluorescence intensity in 10 microaneurysms from two different donors and their adjacent nonaffected capillaries demonstrated that differences in p53 expression were statistically significant. $^{*}P < 0.0005$. *Scale bars* denote **A** = 13.42 μm; **B** = 26.06 μm; and **C** = 18.30 μm.

In contrast to other cell types, such as senescent fibroblast that are resistant to apoptotic stimuli, senescent endothelial cells have increased sensitivity to apoptosis.[42] This was consistent with our observations in retinal endothelial cells from old-age donors where (1) the senescent marker lipofuscin, detected by its autofluorescence emission, was associated with activated caspase 3 (Fig. 12B) and (2) lipofuscin granules were associated with apoptotic bodies,

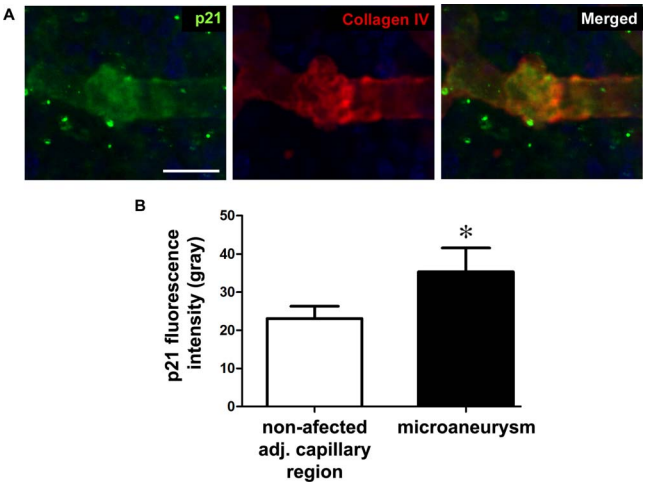

Figure 11. p21 was up-regulated in old-age human retinal microaneurysms. Immunohistochemical detection of p21 (*green*) in whole mount old-age retinas demonstrated an increased expression of this protein in microaneurysms compared with a nonaffected capillary region. Blood vessels were identified by immunohistochemistry with anti-collagen IV antibodies (**A**). (**B**) Quantification of fluorescence intensity in eight microaneurysms from two different donors and their adjacent nonaffected capillaries demonstrated that differences in p21 expression were statistically significant. $^{**}P < 0.05$. *Scale bars* denote **A** = 14.61 μm; **B** = 17.29 μm; and **C** = 16.24 μm.

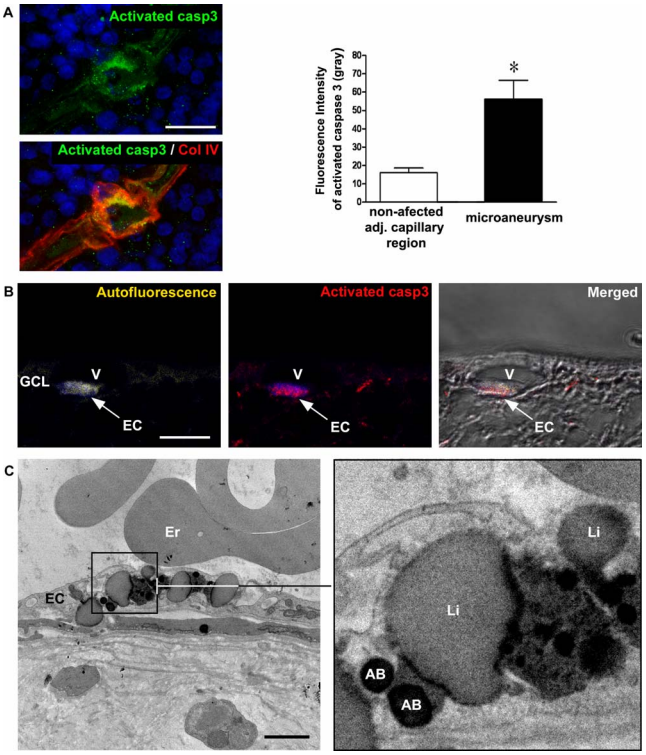

Figure 12. Activated caspase 3 and lipofuscin accumulation coexisted in retinal endothelial cells from old-age donors. (**A**) Microaneurysms, identified as localized dilations of retinal capillaries in collagen IV immunostained whole mount retinas, presented higher levels of activated caspase 3 in comparison with their adjacent nonaffected capillary regions. Nuclei were counterstained with ToPro-3 (*blue*). Quantification of fluorescence intensities in five different microaneurysms and their adjacent capillary regions demonstrated that differences were statistically significant. (**B**) Lipofuscin autofluorescence (*yellow*) coincided with the activated caspase 3 fluorescent signal (*red*) in endothelial cells. Nuclei were counterstained with Hoechst stain (blue). (**C**) At the ultrastructural level, typical lipofuscin granules surrounded by an electrondense crown coexisted in the same endothelial cell with apoptotic bodies, a type of round nuclear heterocromatinic debris, considered a hallmark of apoptosis in transmission electron microscopy. V, blood vessel (venule); EC, endothelial cell; GCL, ganglion cell layer; Er, erythrocyte; AB, apoptotic body; Li, lipofuscin granule; AU, arbitrary units. $^{*}P < 0.05$. *Scale bars* denote **A** (*upper*) = 19.50 μm; **B** = 12.52 μm; and **C** = 1.43 μm.

both visualized by transmission electron microscopy (Fig. 12C).

Senescence and apoptosis pathways could be simultaneously engaged in certain processes or stress responses.[42] In this regard, the p53 senescence marker acts as a nuclear transcription factor that transactivates genes involved in apoptosis, and at the cytoplasmic level, p53 induces mitochondrial outer membrane permeabilization, thereby triggering the release of proapoptotic factors from the mitochondrial intermembrane space.[43] Furthermore, overexpression of p16 induces anoikis, by restoring apoptosis on loss of cellular extracellular anchorage.[44] Anoikis induced by p16 is mediated by the cellular membrane receptor $\alpha_5\beta_1$ integrin that binds extracellular fibronectin.[44] To get further insight into the possible apoptotic function of p16, we analyzed its subcellular localization in old-age human retinal endothelial cells by immunoelectronmicroscopy using a gold-labeled secondary antibody against the anti-p16 antibody. Under transmission electron microscopy, gold beads were found in the inner part of the cellular membrane at the abluminal surface of

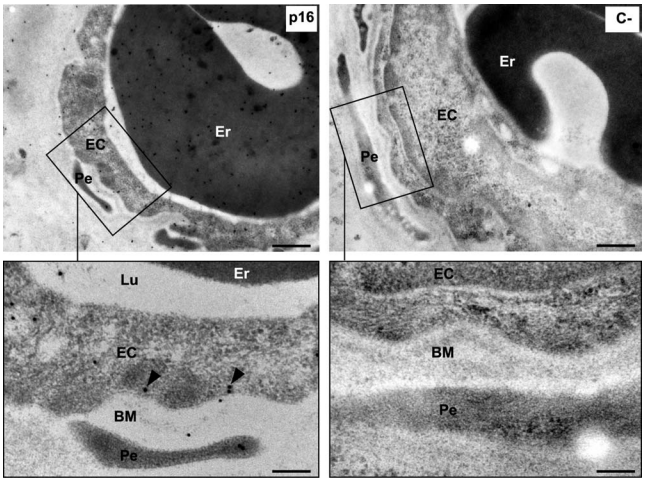

FIGURE 13. p16 was localized under the cellular membrane at the abluminal surface of senescent endothelial cells. Immunoelectronmicroscopy evidenced that p16, labeled with 15-nm gold beads (*arrowheads*), is localized in the cytoplasm of endothelial cells from old-age retinal blood vessels in close contact with their cellular membrane under the basement membrane. As expected, in a negative control where the primary antibody was omitted, gold beads were absent, thus confirming the specificity of p16 labeling. EC, endothelial cell; Er, erythrocyte; Pe, pericyte; Lu, lumen; BM, basement membrane. *Scale bars* denote *left* = 458.58 nm and *right* = 547.48 nm.

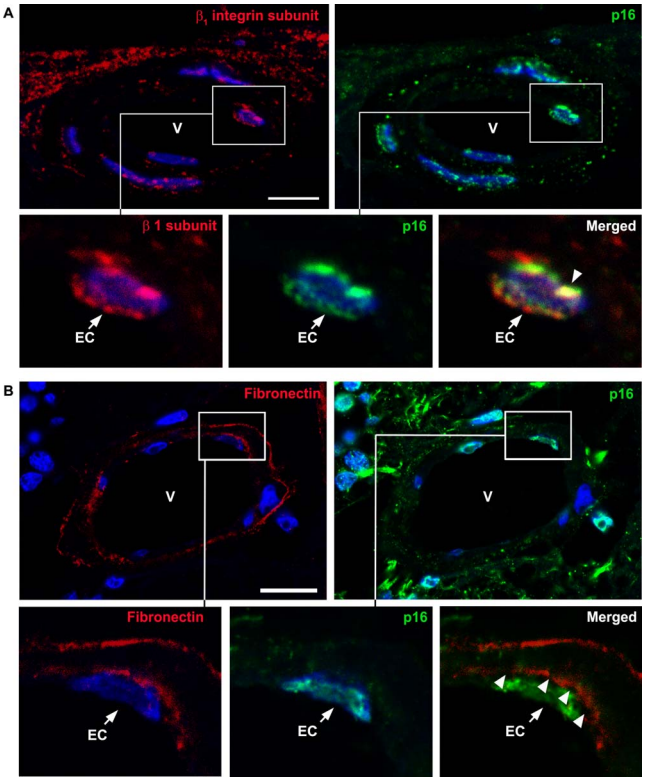

FIGURE 14. Evidence suggesting p16-mediated anoikis in senescent endothelial cells. (**A**) Analysis of immunolabeled retinal paraffin sections by confocal laser microscopy demonstrated that p16 colocalized with the β_1 integrin subunit (*arrowhead*), the intracellular part of the fibronectin receptor (**B**). Fibronectin coating was discontinuous (*arrowheads*) in senescent endothelial cells, evidenced by their specific p16 expression. Nuclei were counterstained with ToPro-3 (*blue*). EC, endothelial cell; v, blood vessel (arteriole). *Scale bars* denote **A** = 7.55 μm and **B** =15.85 μm.

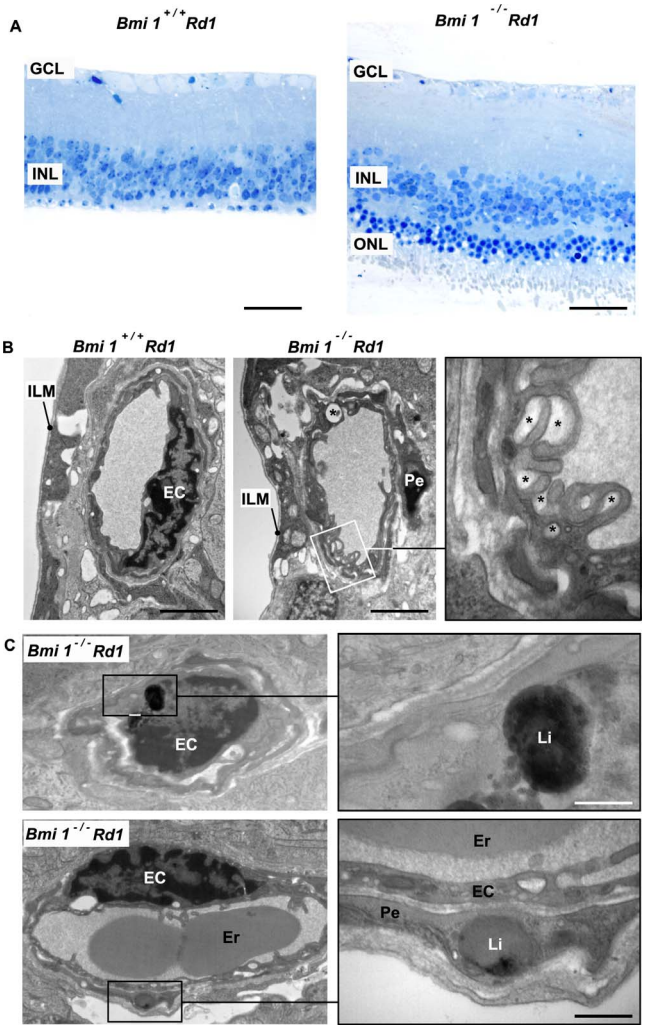

FIGURE 15. Retinal blood vessel aging phenotype in a mouse progeria model deficient in Bmi1. (**A**) Two-month-old *Bmi1*$^{+/+}$ *Rd1* mice showed degeneration of outer nuclear layer, whereas the genetic ablation of *Bmi1* in the *Bmi1*$^{-/-}$ *Rd1* mice provided extensive photoreceptor survival and the outer nuclear layer reappeared. (**B**) Two-month-old *Bmi1*$^{-/-}$ *Rd1* mice showed enlarged caveolae (*asterisks*) in pericytes and endothelial cells. (**C**) Two-month-old *Bmi1*$^{-/-}$ *Rd1* mice accumulated lipofuscin granules in endothelial cells and pericytes of retinal blood vessels. GCL, ganglion cell layer; INL, inner nuclear layer; ONL, outer nuclear layer; EC, endothelial cell; Er, erythrocyte; Pe, pericyte; ILM, internal limiting membrane; Li, lipofuscin granule. *Scale bars* denote **A** = 37.4 μm; **B** = 1.55 μm; **C** (*upper*) = 325.05 nm; and **C** (*lower*) = 341.41 nm.

endothelial cells (Fig. 13), suggesting that p16 was localized under the cellular membrane close to the extracellular matrix that surrounds blood vessels. To know if p16 protein located under the cellular membrane of aged endothelial cells interacts with the $\alpha_5\beta_1$ integrin, a colocalization study between β_1 integrin subunit and p16 was performed by immunohistochemistry and confocal analysis. As shown in Figure 14A, p16 colocalized with the β_1 subunit, suggesting that part of the apoptosis observed in aged retinal endothelial cells could be mediated by the interaction between p16 and the $\alpha_5\beta_1$ integrin. Furthermore, aged endothelial cells overexpressing p16 showed a discontinuous coverage of fibronectin in their abluminal surface (Fig. 14B), pointing to anoikis as a possible type of apoptosis that could occur in human retinal endothelial cells during aging.

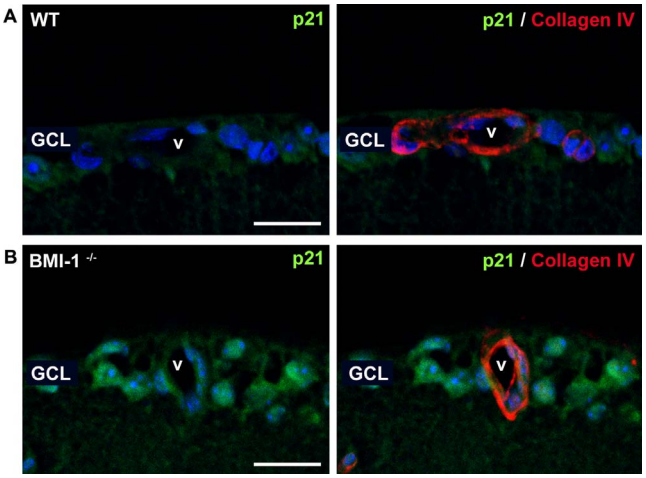

FIGURE 16. p21 is expressed in retinal blood vessels from Bmi1-deficient mice. (**A**) As evidenced by immunohistochemistry in paraffin sections, p21 expression is almost negligible in the wild-type (WT) mouse retina. (**B**) In contrast, retinas from *BMI-1*$^{-/-}$ *Rd1* mice showed an evident expression of p21 in neurons, as well as in endothelial and smooth muscle cells. V, vessel (arteriole); CGL, ganglion cell layer. *Scale bars* denote 18.55 μm.

Retinal Microaneurysms in Progeric Mice

Polycomb group proteins form large multimeric complexes that silence specific target genes by modifying chromatin organization.[45] Bmi1, a member of the Polycomb group family, is down-regulated in old-age human retinas,[46] and inactivation of *Bmi1* in mice induces a premature progeroid-like phenotype in the eye.[47] *Bmi1*$^{-/-}$ mice display cataracts, retinal gliosis, loss of heterochromatin, and necroptosis in photoreceptors.[47,48] Furthermore, *Bmi1* deficiency has been associated with activation of p16 in human and mouse retinas,[47,48] which is consistent with the Bmi1 general function to inhibit the p16/cyclin-dependent kinase 6/retinoblastoma pathway.[49] To get further insight into age-dependent mechanisms involved in microaneurysm formation, retinal blood vessels were analyzed in 2-month-old *Bmi1*$^{-/-}$ mice. *Bmi1*$^{+/+}$ mice carried a mutation in the rod-specific *Phosphodiesterase-6β* gene (*Rd1* mutation) that produces extensive photoreceptor degeneration and loss of the retinal outer nuclear layer (Fig. 15A). In contrast, genetic ablation of *Bmi1* provided extensive photoreceptor survival[50] and the retina of *Bmi1*$^{-/-}$ *Rd1* mice showed the outer nuclear layer of photoreceptors (Fig. 15A). Furthermore, p21 was expressed in blood vessels suggesting that, as happens in humans, retinal blood vessels undergo cellular senescence (Fig. 16).

In 2-month-old *Bmi1*$^{-/-}$ *Rd1* mice, retinal blood vessels displayed an aging phenotype characterized by enlarged caveolae, determining the characteristic "foamy" aspect of aged endothelial cells[9] (Fig. 15B), and accumulation of lipofuscin granules, in both endothelial cells and pericytes (Fig. 15C). Furthermore, the analysis of whole mount retinas immunohistochemically marked with anti-collagen IV showed multiple microaneurysms located in the superficial vascular plexus of *Bmi1*$^{-/-}$ *Rd1* mice (Fig. 17), supporting the idea that cellular senescence could induce the formation of microaneurysms in old-age people.

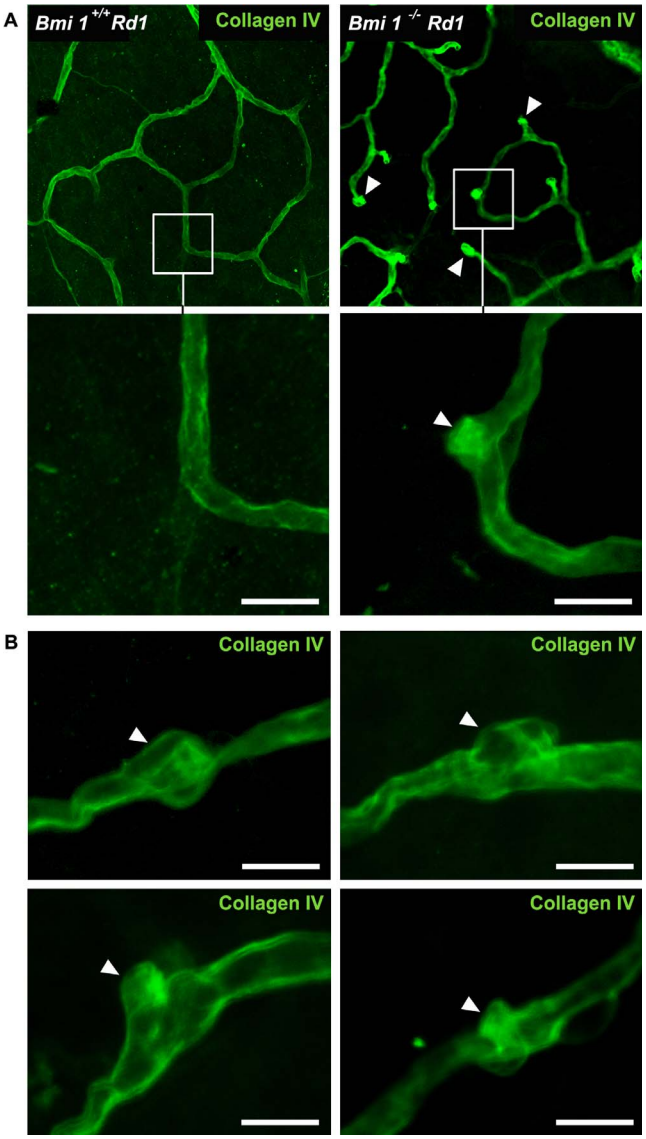

FIGURE 17. Bmi1-deficient mice presented retinal microaneurysms. (**A**) Multiple retinal microaneurysms (*arrowheads*) were found in the superficial vascular plexus of 2-month-old *Bmi1*$^{-/-}$ *Rd1* mice but none could be observed in *Bmi1*$^{+/+}$ *Rd1* retinal vasculature. (**B**) Several examples of microaneurysms (*arrowhead*) found in *Bmi1*$^{-/-}$ *Rd1* retinal blood vessels. Images in **A** and **B** correspond to whole mount retinas immunohistochemically labeled with an anti-collagen IV antibody. *Scale bars* denote 50 μm.

Discussion

Fifty-five years ago, L. Hayflick and P. Moorhead observed that human fibroblasts exhibited a limited proliferative capacity in culture, a phenomenon that they named "cellular senescence," and speculated that it could be a cause of aging.[51] Here, our results confirm and extend a preliminary study that report cellular senescence during human retinal aging.[46] The canonical senescence biomarker p16 was 12-fold overexpressed in old-age retinas compared with middle-age retinas, supporting a correlation between cellular levels of p16 and the chronological age of essentially all tissues analyzed.[52,53] Our results also showed that neurons but not neuroglial cells undergo cellular senescence during retinal aging.

Cellular senescence has been implicated in age-dependent eye diseases, such as AMD[54,55] and more recently glaucoma.[56] Furthermore, cellular senescence has been associated with several vascular diseases, including the formation of brain and coronary aneurysms.[20,21] Here, we report that retinal microaneurysms overexpress p16, p53, and p21, suggesting that

Investigative Ophthalmology & Visual Science

cellular senescence is associated with the pathogenesis of this lesion. Cell death and apoptosis, mechanisms also associated with microaneurysm formation during diabetic retinopathy,[11] co-occur with cellular senescence in old-age retinal microaneurysms from nondiabetic donors.

Although described in some mouse models, such as VEGF transgenic Kimba mice[57] and plateled-derived growth factor (PDGF)-β endothelium restricted–deficient mice,[58] microaneurysms do not generally develop in mouse retina. It has been suggested that this may be caused by the presence of precapillary sphincters, which probably protect capillary beds from hypertensive injury.[59] In this context, it is relevant that, despite how little the mouse retina is prone to develop microaneurysms, a progeric mouse that overexpress p21 in retinal blood vessels displays this lesion. In our opinion, this fact reinforces the hypothesis that cellular senescence is a mechanism associated with retinal microaneurysm formation in aging.

Meta-analysis of more than 300 genome-wide association studies identified the INK4a/ARF locus, which encodes p16, as the genomic locus that is genetically linked to the highest number of age-associated pathologies, including type 2 diabetes.[60] Furthermore, pancreatic β cell senescence has been identified as a player that contributes to the pathogenesis of type 2 diabetes.[61] These observations, together with the similarities noted between our study using nondiabetic old-age donors and previous studies using diabetic donors,[3,10,11,14] could suggest that cellular senescence is a common cause for the development of retinal microaneurysms in both diabetic and aging conditions. Further studies must be launched in the future to enlighten this possibility.

Acknowledgments

The authors thank Manuel Serrano for his valuable comments. The authors also thank Veronica Melgarejo, Lorena Noya, and Angel Vazquez for technical assistance.

Supported by grants from Instituto de Salud Carlos III (PI12/00605 and PI16/00719), Spain; Gundação para a Ciência e a Tecnologia (SFRH/BPD/102573/2014), Ministerio da Educação e Ciência, Portugal; and Fondo Europeo de Desarrollo Regional (FEDER).

Disclosure: **M. López-Luppo**, None; **J. Catita**, None; **D. Ramos**, None; **M. Navarro**, None; **A. Carretero**, None; **L. Mendes-Jorge**, None; **P. Muñoz-Cánoves**, None; **A. Rodriguez-Baeza**, None; **V. Nacher**, None; **J. Ruberte**, None

References

1. Uiker S, Kriz W. Structural analysis of the formation of glomerular microaneurysms in the Habu venom model. *Virchows Arch*. 1995;426:281–293.
2. Balofsky A. Microaneurysms in the diabetic human heart. *Isr Med Assoc J*. 2010;12:391.
3. Stitt AW, Gardiner TA, Archer DB. Histological and ultrastructural investigation of retinal microaneurysm development in diabetic patients. *Br J Ophthalmol*. 1995;79:362–367.
4. Moore J, Bagley S, Irelanda G, McLeod D, Boulton ME. Three dimensional analysis of microaneurysms in the human diabetic retina. *J Anat*. 1999;194(Pt 1):89–100.
5. Gardiner TA, Archer DB, Curtis TM, Stitt AW. Arteriolar involvement in the microvascular lesions of diabetic retinopathy: implications for pathogenesis. *Microcirculation*. 2007; 14:25–38.
6. Curtis TM, Gardiner TA, Stitt AW. Microvascular lesions of diabetic retinopathy: clues towards understanding pathogenesis? *Eye*. 2009;23:1496–1508.
7. Dubow M, Pinhas A, Shah N, et al. Classification of human retinal microaneurysms using adaptive optics scanning light ophthalmoscope fluorescein angiography. *Invest Ophthalmol Vis. Sci*. 2014;55:1299–1309.
8. Sugi K. Studies on the pathological changes in the retinal vessels of human eyes, using the trypsin digestion method. *Jap J Ophthalmol*. 1966;10:252–259.
9. Catita J, López-Luppo M, Ramos D, et al. Imaging of cellular aging in human retinal blood vessels. *Exp Eye Res*. 2015;135: 14–25.
10. Friedenwald JS. Diabetic retinopathy. *J Am Med Assoc*. 1952; 150:969–971.
11. Cogan DG, Kuwabara T. The mural cell in perspective. *Arch Ophthalmol*. 1967;78:133–139.
12. Wise GN. Retinal microaneurysms. *Trans Am Ophthalmol Soc*. 1956;57:151–156.
13. Little HL, Sachs AH. Role of abnormal blood rheology in the pathogenesis of diabetic retinopathy. *Trans Sect Ophthalmol Am Acad Ophthalmol Otolaryngol*. 1977; 83(Pt 1):OP522–OP534.
14. Frank RN. On the pathogenesis of diabetic retinopathy. *Ophthalmology*. 1984;91:626–634.
15. Campisi J, d'Adda di Fagagna F. Cellular senescence: when bad things happen to good cells. *Nat Rev Mol Cell Biol*. 2007;8: 729–740.
16. Collado M, Blasco MA, Serrano M. Cellular senescence in cancer and aging. *Cell*. 2007;130:223–233.
17. Kuilman T, Michaloglou C, Mooi WJ, Peeper, DS. The essence of senescence. *Genes Dev*. 2010;24:2463–2479.
18. Muñoz-Espín D, Serrano M. Cellular senescence: from physiology to pathology. *Nat Rev Mol Cell Biol*. 2014;15: 482–496.
19. Rodier F, Campisi J. Four faces of cellular senescence. *J Cell Biol*. 2011;192:547–556.
20. Fukazawa R, Ikegam E, Watanabe M, et al. Coronary artery aneurysm induced by Kawasaki disease in children show features typical senescence. *Circ J*. 2007;71:709–715.
21. Wei H, Mao Q, Liu L, et al. Changes and function of circulating endothelial progenitor cells in patients with cerebral aneurysm. *J Neurosci Res*. 2011;89:1822–1828.
22. Nacher V, Carretero A, Navarro M, et al. The quail mesonephros: a new model for renal senescence? *J Vasc Res*. 2006;43:581–586.
23. Kim WY, Sharpless NE. The regulation of INK4/ARF in cancer and aging. *Cell*. 2006;127:265–275.
24. López-Otín C, Blasco MA, Partridge L, Serrano M, Kroemer G. The hallmarks of aging. *Cell*. 2013;153:1194–1216.
25. Mahajan A. Practical issues in the application of p16 immunohistochemistry in diagnostic pathology. *Hum Pathol*. 2016;51:64–74.
26. Loeffler KU, Mangini NJ. Immunolocalization of ubiquitin and related enzymes in human retina and retinal pigment epithelium. *Graefes Arch Clin Exp Ophthalmol*. 1997;235: 248–254.
27. Kivela T, Tarkkanen A, Virtanen I. Intermediate filaments in the human retina and retinoblastoma. An immunohistochemical study of vimentin, glial fibrillary acidic protein, and neurofilaments. *Invest Ophthalmol Vis Sci*. 1986;27:1075–1084.
28. de Souza CF, Nivison-Smith L, Christie DL, et al. Macromolecular markers in normal human retina and applications to human retinal disease. *Exp Eye Res*. 2016;150:135–148.
29. Ljubimov AV, Burgeson RE, Butkowski RJ, et al. Basement membrane abnormalities in human eyes with diabetic retinopathy. *J Histochem Cytochem*. 1996;44:1649–1479.

30. Kawai M, Ogawa Y, Shimmura S, et al. Expression and localization of aging markers in lacrimal gland of chronic graft-versus-host disease. *Sci Rep*. 2013;3:2455.
31. Rodriguez-Menocal L, Pham SM, Mateu D, et al. Aging increases $p16^{INK4a}$ in vascular smooth-muscle cells. *Biosci Rep*. 2009;30:11–18.
32. Dimri GP, Lee X, Basile G, et al. A biomarker that identifies senescent human cells in culture and in aging skin in vivo. *Proc Natl Acad Sci U S A*. 1995;92:9363–9365.
33. Georgakopoulou EA, Tsimaratou K, Evangelou K, et al. Specific lipofuscin staining as a novel biomarker to detect replicative and stress-induced senescence. A method applicable in cryo-preserved and archival tissues. *Aging*. 2013;5:37–50.
34. Kurz DJ, Decary S, Hong Y, Erusalimsky JD. Senescence-associated (beta)-galactosidase reflects an increase in lysosomal mass during replicative ageing of human endothelial cells. *Cell Sci*. 2000;113(Pt 20):3613–3622.
35. Feeney L. Lipofuscin and melanin of human retinal pigment epithelium. Fluorescence, enzyme cytochemical, and ultrastructural studies. *Invest Ophthalmol Vis Sci*. 1978;17:583–600.
36. Katz ML, Robison WG Jr. What is lipofuscin? Defining characteristics and differentiation from other autofluorescent lysosomal storage bodies. *Arch Gerontol Geriatr*. 2002;34:169–184.
37. Jung T, Bader N, Grune T. Lipofuscin: formation, distribution, and metabolic consequences. *Ann NY Acad Sci*. 2007;1119:97–111.
38. Young AR, Narita M, Ferreira M, et al. Autophagy mediates the mitotic senescence transition. *Genes Dev*. 2009;23:798–803.
39. Lamark T, Kirkin V, Dikic I, Johansen T. NBR1 and p62 as cargo receptors for selective autophagy of ubiquitinated targets. *Cell Cycle*. 2009;8:1986–1990.
40. Sasaki M, Miyakoshi M, Sato Y, Nakanuma Y. A possible involvement of p62/sequestosome-1 in the process of biliary epithelial autophagy and senescence in primary biliary cirrhosis. *Liver Int*. 2012;32:487–499.
41. Namura S, Zhu J, Fink K, et al. Activation and cleavage of caspase-3 in apoptosis induced by experimental cerebral ischemia. *J Neurosci*. 1998;18:3659–3668.
42. Childs BG, Baker DJ, Kirkland JL, Campisi J, Van Deursen JM. Senescence and apoptosis: dueling or complementary cell fates? *EMBO Rep*. 2014;15:1139–1153.
43. Green DR, Kroemer G. Cytoplasmic funcions of the tumour supressor p53. *Nature*. 2009;458:1127–1130.
44. Plath T, Detjen K, Welzel M, et al. A novel function for the tumor supressor $p16^{INK4a}$: induction of anoikis via upregulation of the $\alpha_5\beta_1$ fibronectin receptor. *J Cell Biol*. 2000;150:1467–1477.
45. Valk-Lingbeek ME, Bruggeman SW, Van Lohuizen M. Stem cells and cancer: the polycomb connection. *Cell*. 2004;118:409–418.
46. Abdouh M, Chatoo W, Hajjar JE, David J, Ferreira J. Bmi1 is down-regulated in the aging brain and displays antioxidant and protective activities in neurons. *PLoS One*. 2012;7:e31870.
47. Chatoo W, Abdouh M, David J, et al. The polycomb group gene Bmi1 repressing p53 pro-oxidant activity. *J Neurosci*. 2009;29:529–542.
48. Barabino A, Plamondon V, Abdouh M, et al. Loss of Bmi1 causes anomalies in retinal development and degeneration of cone photoreceptors. *Development*. 2016;143:1571–1584.
49. Sauvageau M, Sauvageau G. Polycomb group proteins multi-faceted regulators of somatic stem cells and cancer. *Cell Stem Cell*. 2010;7:299–313.
50. Zenkac D, Schouwey K, Chen K, et al. Retinal degeneration depends on Bmi1 function and reactivation of cell cycle proteins. *Proc Natl Acad Sci U S A*. 2013;110:E593–E601.
51. Hayflick L, Moorhead PS. The serial cultivation of human diploid cell strains. *Exp Cell Res*. 1961;25:585–621.
52. Krishnamurthy J, Torrice C, Ramsey MR, et al. Ink4a/Arf expression is a biomarker of aging. *J Clin Invest*. 2004;114:1299–1307.
53. Ressler S, Bartkova J, Niederegger H, et al. p16INK4A is a robust in vivo biomarker of cellular aging in human skin. *Aging Cell*. 2006;5:379–389.
54. Mishima KI, Handa JT, Aotaki-Keen A, Lutty GA, Morse LS, Hjelmeland LML. Senescence-associated beta-galactosidase histochemistry for the primate eye. *Invest Ophthalmol Vis Sci*. 1999;40:1590–1593.
55. Zhu D, Wu J, Spee C, Ryan SJ, Hinton DR. BMP4 mediates oxidative stress-induced retinal pigment epithelial cell senescence and is overexpressed in age-related macular degeneration. *J Biol Chem*. 2009;284:9529–9539.
56. Skowronska-Krawczyk D, Zhao L, Zhu J, et al. P16INK4a upregulation mediated by SIX6 defines retinal ganglion cell pathogenesis in glaucoma. *Mol Cell*. 2015;59:931–940.
57. Lai CM, Dunlop SA, May LA, et al. Generation of transgenic mice with mild and severe retinal neovascularisation. *Br J Ophthalmol*. 2005;89:911–916.
58. Enge M, Bjarnegård M, Gerhardt H, et al. Endothelium-specific platelet-derived growth factor-B ablation mimics diabetic retinopathy. *EMBO J*. 2002;21:4307–4316.
59. Curtis TM, Gardiner TA, Stitt AW. Microvascular lesions of diabetic retinopathy: clues towards understanding pathogenesis. *Eye*. 2009;23:1496–1508.
60. Jeck WR, Siebold AP, Sharpless NE. Review: a meta-analysis of GWAS and age-associated diseases. *Aging Cell*. 2012;11:727–731.
61. Sone H, Kagawa Y. Pancreatic beta cell senescence contributes to the pathogenesis of type 2 diabetes in high-fat diet-induced diabetic mice. *Diabetologia*. 2005;48:58–67.

Investigative Ophthalmology & Visual Science